NASA TECHNICAL MEMORANDUM

NASA TM X-2873

NASA TM X-2873

EFFECTS OF FLAPS ON BUFFET CHARACTERISTICS AND WING-ROCK ONSET OF AN F-8C AIRPLANE AT SUBSONIC AND TRANSONIC SPEEDS

by Richard C. Monaghan and Edward L. Friend

Flight Research Center
Edwards, Calif. 93523

NATIONAL AERONAUTICS AND SPACE ADMINISTRATION • WASHINGTON, D. C. • AUGUST 1973

1. Report No. NASA TM X-2873	2. Government Accession No.	3. Recipient's Catalog No.
4. Title and Subtitle EFFECTS OF FLAPS ON BUFFET CHARACTERISTICS AND WING-ROCK ONSET OF AN F-8C AIRPLANE AT SUBSONIC AND TRANSONIC SPEEDS		5. Report Date August 1973 6. Performing Organization Code
7. Author(s) Richard C. Monaghan and Edward L. Friend		8. Performing Organization Report No. H-742 10. Work Unit No. 766-73-02-00
9. Performing Organization Name and Address NASA Flight Research Center P. O. Box 273 Edwards, California 93523		11. Contract or Grant No. 13. Type of Report and Period Covered Technical Memorandum
12. Sponsoring Agency Name and Address National Aeronautics and Space Administration Washington, D. C. 20546		14. Sponsoring Agency Code
15. Supplementary Notes		

16. Abstract

Wind-up-turn maneuvers were performed to establish the values of airplane normal force coefficient for buffet onset, wing-rock onset, and buffet loads with various combinations of leading- and trailing-edge flap deflections. Data were gathered at both subsonic and transonic speeds covering a range from Mach 0.64 to Mach 0.92. Buffet onset and buffet loads were obtained from wingtip acceleration and wing-root bending-moment data, and wing-rock onset was obtained from airplane roll rate data.

Buffet onset, wing-rock onset, and buffet loads were similarly affected by the various combinations of leading- and trailing-edge flaps. Subsonically, the 12° leading-edge-flap and trailing-edge-flap combination was most effective in delaying buffet onset, wing-rock onset, and equivalent values of buffet loads to a higher value of airplane normal force coefficient. This was the maximum flap deflection investigated. Transonically, however, the optimum leading-edge flap position was generally less than 12°.

17. Key Words (Suggested by Author(s))	18. Distribution Statement
Buffet, F-8C Wing rock, F-8C Buffet, F-8C with flaps	Unclassified - Unlimited

19. Security Classif. (of this report)	20. Security Classif. (of this page)	21. No. of Pages	22. Price*
Unclassified	Unclassified	27	$3.00

*For sale by the National Technical Information Service, Springfield, Virginia 22151

EFFECTS OF FLAPS ON BUFFET CHARACTERISTICS AND WING-ROCK ONSET OF AN F-8C AIRPLANE AT SUBSONIC AND TRANSONIC SPEEDS

Richard C. Monaghan and Edward L. Friend
Flight Research Center

INTRODUCTION

To achieve maneuver objectives within the subsonic and transonic flight envelope, fighter aircraft frequently must fly under conditions of sustained buffet caused by flow separation over the wing. Flight under conditions of separated flow may cause significant structural, performance, and handling qualities problems in the form of structural damage due to high buffet loads, increased power requirements due to flow separation drag, and wing rock and other control difficulties due to unsymmetrical wing flow separation. Because of these problems, it is desirable to delay either flow separation or the increase in buffet loads to as high an airplane normal force coefficient as possible.

Results of wind-tunnel tests indicate that changes in wing sweep or changes in airfoil section through flap deflection improve aircraft buffet characteristics at subsonic and transonic Mach numbers (ref. 1).

Several flight-test programs were undertaken to verify the wind-tunnel findings (refs. 2 to 4). References 3 and 4 indicate that improvements in the buffet characteristics of several aircraft can be achieved by deflecting the leading-edge flaps, the trailing-edge flaps, or both. Most of the data in references 3 and 4 were obtained from F-111 and F-104 aircraft.

An F-8C airplane was selected as the test vehicle to further the investigation of the effects of wing leading- and trailing-edge flaps on buffet onset, wing-rock onset, and buffet loads. The F-8C airplane has a moderate aspect ratio (3.4) and a moderate wing thickness (5.5 percent), and it is designed to operate and maneuver effectively at high altitudes and transonic speeds. The airplane also provides a full range of flap deflections without limiting the flight envelope at the desired test conditions.

Presented in this report are data from wind-up-turn maneuvers which were performed with various combinations of leading- and trailing-edge flap deflections at Mach numbers between 0.64 and 0.92. Comparisons are made between data for subsonic and transonic Mach numbers for buffet onset, wing-rock onset, buffet loads, and power spectral densities. Wind-tunnel buffet-onset data for the clean-wing configuration are presented and compared with data obtained in flight.

SYMBOLS

Physical quantities in this report are given in the International System of Units (SI) and parenthetically in U.S. Customary Units. The measurements were taken and the calculations were made in U.S. Customary Units. Factors relating the two systems are presented in reference 5.

$a_{n_{cg}}$	center of gravity normal acceleration, g units
$a_{n_{cp}}$	cockpit normal acceleration, g units
$a_{n_{wt}}$	wingtip normal acceleration, g units
B_w	wing bending moment at wing strain-gage location, m-N (in-lb)
C_L	airplane lift coefficient
C_{N_A}	airplane normal force coefficient, $\frac{a_{n_{cg}} W}{qS}$
f	frequency, Hz
M	Mach number
p	roll rate, deg/sec
q	free-stream dynamic pressure, N/m^2 (lb/ft^2)
q_{ref}	reference free-stream dynamic pressure used for normalizing unsteady acceleration and bending-moment data, N/m^2 (lb/ft^2)
r	yaw rate, deg/sec
S	wing reference area, 34.8 m^2 (375 ft^2)
W	airplane weight, kg (lb)
α	airplane true angle of attack, deg
β	airplane angle of sideslip, deg
σ	root mean square value of associated quantity
Φ	power spectral density of associated quantity

Subscript:

i	indicated gage output

ABBREVIATIONS

L.E.	leading edge, deg
PCM	pulse code modulation
rms	root mean square
T.E.	trailing edge, deg

AIRPLANE DESCRIPTION

The F-8C airplane (fig. 1) is a single-place carrier- or land-based aircraft which is powered by an afterburning turbojet engine and is capable of maneuvering at high altitudes. It is characterized by a thin, sweptback wing which has two incidence angle positions and is mounted high on the fuselage. The greater angle of incidence is used during takeoff and landing. The wings incorporate full-span leading-edge flaps and partial-span ailerons located inboard on the wings which also serve as takeoff and landing flaps (fig. 2). Pertinent wing dimensions and physical characteristics are presented in table 1.

The pilot was provided with a trailing-edge flap position switch that enabled him to select specific flap positions during flight. The position of the leading-edge flap could also be selected during flight, except for the 12° deflection. The flap was secured in this position before takeoff and remained fixed throughout the flight.

Airplane roll control was supplemented by spoilers on the upper surface of the wing. The spoiler was first activated when the aileron was positioned approximately 1.5° above the faired-wing position, and it opened to a maximum of 49° when the aileron was 15° up.

INSTRUMENTATION AND RECORDING

Of the parameters for which the F-8C airplane was instrumented, the following are pertinent to this study:

- Airspeed
- Altitude
- Airplane angle of attack
- Airplane angle of sideslip
- Wingtip acceleration
- Wing-root bending moment
- Pilot compartment normal acceleration
- Center of gravity normal acceleration
- Roll rate
- Yaw rate

A standard NASA airspeed head (ref. 6), angle of attack vane, and angle of sideslip vane were located on a boom mounted on the airplane's nose. Angle of attack and angle of sideslip were measured relative to the fuselage reference line.

Wing bending moment was measured by using semiconductor gages (ref. 7), which for equivalent loads produce much higher gage outputs than conventional strain gages. The outputs of the wingtip accelerometer and wing bending-moment gage (fig. 2) were high pass filtered at 3 hertz to eliminate gage response due to maneuver loads. The recording system acted as a filter above 40 hertz. These filters, used in conjunction with the wingtip accelerometers and the wing bending gages, produced data of greater resolution in the range of the frequencies of interest. The cockpit and the center of gravity accelerometers were mounted on major structural members near the pilot's seat and near the center of gravity, respectively. Rate gyros were used to measure roll and yaw rates.

To facilitate data reduction, a pulse code modulation (PCM) system was utilized. This system was composed of an airborne PCM encoder, a telemetry transmitter, and a ground-based telemetry receiver coupled with a tape recorder and display equipment so that a permanent record of the flight data could be obtained in digital form on tape and so that a real-time analog display record could be viewed during flight.

The errors in the unsteady flow response parameters associated with the instrumentation and recording system were considered negligible with respect to the data scatter.

Angle of attack as used in this report was corrected for upwash and had an accuracy of $\pm 0.25^\circ$. The normal force coefficient had an accuracy of approximately ± 0.03.

FLIGHT-TEST CONDITIONS

The F-8C airplane was tested for nine combinations of leading- and trailing-edge flap deflections in the subsonic and transonic Mach number ranges. Trailing-edge deflections of 0°, 8°, and 12° and leading-edge deflections of 0°, 7°, and 12° were used in various combinations. Data were gathered for Mach numbers from 0.64 to 0.92 at a dynamic pressure of 14,400 newtons per square meter (300 pounds per square foot). Emphasis was placed on the Mach number ranges from 0.65 to 0.70 and 0.85 to 0.90, which were considered to represent a subsonic and a transonic flight condition, respectively. All the data were obtained from wind-up-turn maneuvers with the wing fuel tanks empty. Airplane gross weight varied from 9070 to 9980 kilograms (20,000 to 22,000 pounds) during test maneuvers. The wing spoilers were activated by aileron deflections of approximately 1.5° and greater above the faired-wing position. This condition occurred during test maneuvers performed with 0° of trailing-edge flap deflection but not during those with 8° or 12° flap deflections.

DATA INTERPRETATION AND ANALYSIS

Figure 3 presents typical time history plots illustrating buffet and wing-rock characteristics. Buffet onset and wing-rock onset were selected from these and similar traces. The wingtip accelerometer and the wing bending gage gave the best indication of the response of the aircraft structure to buffeting. The pilot compartment accelerometer and the center of gravity accelerometer were sensitive to engine inlet vibration and afterburner operation, which made the selection of wing buffet onset from these instruments unreliable. The data in figure 3 illustrate the problem.

Buffet onset was defined as the first sustained response of the structure to flow separation as indicated by the time history trace of the wingtip accelerometer (fig. 3). This onset criterion was somewhat arbitrary, and it may differ from that used in the past by investigators using different instrumentation or sensor locations (such as center of gravity or pilot compartment accelerometers). Specifically, this definition differs from the definition used in reference 3, where buffet onset was defined as a level of ±0.08g root mean square (rms) at the pilot compartment. Inasmuch as the objective of this study was to determine the conditions for the earliest flow separation on the wing, use of the wingtip accelerometer was felt to be appropriate. The wing bending-moment gage responded slightly later than the wingtip accelerometer, as can be seen in figure 3.

Roll rate, yaw rate, and angle of sideslip gave an indication of the response of the airplane to wing rock. Wing rock was defined as a lateral-directional oscillation induced primarily by separated flow on the wing at high angles of attack (ref. 8). Wing-rock-onset points were determined from the time history record, which showed the onset as a sustained oscillation in roll. Only those points which preceded significant pilot inputs were chosen.

Buffet load data were calculated and are presented as rms values of the dynamic response of the wingtip accelerometer and wing bending-moment gage. Root mean square values were calculated for each maneuver for selected 1-second intervals from before buffet onset to the point of maximum airplane normal force coefficient.

These rms values were corrected for dynamic pressure variations by the equation

$$\sigma B_w = \frac{\sigma B_{w_i}}{\sqrt{q/q_{ref}}}$$

or

$$\sigma a_{n_{wt}} = \frac{\sigma a_{n_{wt_i}}}{\sqrt{q/q_{ref}}}$$

and were plotted versus C_{N_A} for each flap configuration within a specific range of Mach numbers. When data from several maneuvers for a given configuration fell within the Mach number range selected for analysis, they were combined to form one buffet load curve.

Power spectral density techniques were used to determine the power and frequency distribution of the response of the buffet instrumentation. Time segments of 3 seconds were chosen for analysis from the time history plots. These segments were chosen from periods of constant high intensity buffet. The data were analyzed at 100 samples per second. Since the power spectral density data were derived from relatively short time segments, the results of the analysis were usable only for the comparison of trends among the different wing flap configurations and Mach numbers.

The buffet data in this report are presented with respect to C_{N_A}. Figure 4 is presented in terms of C_{N_A} versus α for a conversion to airplane angle of attack.

RESULTS AND DISCUSSION

Buffet-Onset Boundary

The buffet-onset boundary for each of the nine configurations investigated is shown in figure 5 in terms of C_{N_A} versus Mach number. From this figure it can be seen that at subsonic speeds the deflection of the leading-edge flap caused a large increase in C_{N_A} for buffet onset. With constant leading-edge deflection, the deflection of the trailing-edge flap caused a significant but somewhat smaller increase.

Transonically (near Mach 0.90), a moderate (7°) leading-edge flap deflection raised the C_{N_A} buffet boundary, although much less than it did subsonically. With the highly deflected (12°) leading-edge flap, the C_{N_A} for buffet onset was actually lower than with the leading edge deflected 7°. The trailing-edge flap remained effective transonically when used alone; however, with 7° of leading-edge deflection, deflecting the trailing edge caused little improvement, and with the leading-edge flap deflected 12°, deflecting the trailing edge was actually detrimental. Transonically, 7° of leading-edge flap deflection combined with 12° of trailing-edge flap deflection was most effective in delaying buffet onset to a higher C_{N_A}. For all wing flap combinations, the C_{N_A} for buffet onset was lower transonically than subsonically.

Figure 6 presents clean-wing normal force coefficients for several buffet-onset criteria applied to an F-8C airplane and a 0.042-scale model of the F-8 (ref. 9).

Measurements of unsteady wing bending moments were made for both the model and the airplane. The criterion for buffet onset for the wing bending-moment data for both the model and the airplane was defined as the point of divergence of the rms value of the wing bending moment. Flight bending-moment data indicated a significantly higher C_{N_A} for buffet onset than the model bending-moment data and correlated closely with the curve for the model that indicated the break in the lift coefficient versus angle of attack. Use of the bending moment and the break in the lift curve as criteria for buffet onset resulted in normal force coefficients greater than the value used to define buffet onset in this report, which was based on the wingtip accelerometer. Only the model trailing-edge pressure divergence criterion resulted in a lower C_{N_A} for buffet onset.

Power Spectral Density of Structural Response to Buffeting

Power spectral density analyses of typical wing bending gage data and wingtip accelerometer data are presented in figures 7(a) to 7(c). Both subsonic and transonic Mach number data are shown for three combinations of leading- and trailing-edge flaps. These power spectral density analyses were made using a relatively small number of data points and were therefore used only for the comparison of similar data. Presented in the figures are values for the aircraft natural vibration frequencies as determined by ground vibration tests. It is apparent from the figures that the predominant response of the wing structure to buffet at the location of the wing bending gage occurred at a frequency near that determined in the ground vibration tests for wing first bending. The predominant response of the wingtip accelerometer occurred at a frequency between that determined for wing second bending and wing first torsional frequencies. The wingtip accelerometer also showed some response at the first wing bending frequency, and the wing bending gage responded slightly at a frequency between the wing second bending and first torsional. The power spectral density for the wingtip accelerometer shown in figure 7(b) for the higher Mach number indicated a significant response at 29 hertz. The reason for this peak is not known, but it may have been due to the combination of those particular leading- and trailing-edge flap deflections and flight conditions.

Buffet Loads

Buffet load data are shown in figure 8 for each flap setting investigated. Data are presented for Mach numbers of 0.65 to 0.70 and 0.85 to 0.90, which represent a subsonic condition and a transonic condition, respectively. Because of limited 12° leading-edge data, some of the points for this condition were allowed to fall outside the transonic and subsonic Mach number ranges specified for the other flap configurations by as much as ± 0.04 in Mach number. These points are indicated by the flagged symbols.

Because of the large amount of scatter in the high buffet intensity data (fig. 8), fairing the data was difficult. After examining all the data, it was determined that a reasonable way to fair the data was to use a constant slope within a constant Mach

number range for each configuration. The faired lines agree reasonably well with all the data. The method used is based on the assumption that the rate of intensity rise was constant at a given Mach number.

The values of buffet onset and wing-rock onset selected from time history plots are noted on the buffet load curves in figure 8. Although the values of buffet onset and wing-rock onset were not determined from the data in this figure, they do correspond closely to significant changes in the characteristics of the data. The buffet-onset boundary selected generally falls near the first indication in the data of a sustained rise in buffet intensity. Wing-rock onset occurs at a higher intensity level, in the area of significant data scatter.

High accelerations were observed at the wingtip. Root mean square values were measured that were as high as 6g subsonically and 5g transonically. These large accelerations could have created severe local structural loads. However, the structure was displaced only a small amount because of the high frequency at which it responded, and these small displacements do not necessarily cause severe loading at locations remote from the accelerometer. This appears to have been the case at the wing bending gage location, where there was little power at the high frequency associated with the wingtip accelerations. The maximum rms values of buffet load during the flight reached approximately 10 percent of the 1g steady state flight bending-moment loads at the same location.

The maximum buffet load presented for each wing flap configuration does not necessarily indicate the maximum load attained. At high load factors it was difficult to maintain steady flight conditions, and much of the data fell outside the Mach number range or the dynamic pressure range selected for analysis, or both. In all the data gathered throughout the program, the maximum buffet load attained was approximately the same for all the flap positions tested, even though the maximum C_{N_A} increased significantly with deflected flaps.

The fairings in figure 9 summarize the wingtip accelerometer data presented in figure 8. Only the results from the wingtip accelerometer are summarized because at a constant Mach number the trend of the wing bending-moment data and the wingtip accelerometer data was the same. With increasing flap deflection, the trend of the buffet load data was similar to that of the buffet-onset data. Subsonically (fig. 9(a)), increasing the deflection of either the leading-edge or the trailing-edge flap to the limits investigated resulted in an increase in C_{N_A} for any given value of buffet load. Transonically (fig. 9(b)), the deflection of the trailing-edge flap or the moderate deflection (7°) of the leading-edge flap resulted in an increase in C_{N_A} for any given value of buffet load. With the leading-edge flap deflected 12°, improvements were noted in comparison with the undeflected leading-edge flap configuration, but a decrease in C_{N_A} for any given value of buffet load was realized with respect to the moderately deflected (7°) leading-edge flap configuration. Transonically, 7° of leading-edge flap deflection combined with 12° of trailing-edge flap deflection was the most effective flap combination investigated in terms of delaying equivalent values of buffet loads to a higher C_{N_A}.

The data presented in figure 10 show the effect of Mach number on buffet loads at the wingtip accelerometer. Fairings of the data in figure 8 are shown for subsonic and transonic Mach numbers for wing flap configurations of 0° of both leading- and trailing-edge flap and 7° of leading-edge flap with 12° of trailing-edge flap. The wingtip accelerometer data indicated that the rise in buffet intensity occurred at a lower C_{N_A} transonically than subsonically. The wing bending-moment data in figure 8 also showed this trend.

The wingtip accelerometer indicated that there was a slower rise in buffet intensity with increasing C_{N_A} transonically than subsonically. As C_{N_A} increased within the available data range, the difference in the values of buffet intensity for the subsonic and transonic data decreased. This trend may also have occurred to a lesser degree in the bending-moment data. However, because of the scatter in the data no definite trend could be established.

Wing-Rock Onset

Figure 11 presents the boundaries for wing-rock onset in terms of C_{N_A} versus Mach number for each of the nine wing flap configurations investigated.

For equivalent flight conditions and aircraft configurations, the wing-rock onset boundaries occurred at considerably higher normal force coefficients than the buffet-onset boundaries (C_{N_A} was 0.2 to 0.4 greater). Wing-rock onset, like buffet onset, is a phenomenon of flow separation, and, as shown in figure 3, its occurrence corresponded to a detectable change in buffet intensity. Time histories similar to the one shown in figure 3 and the buffet load data in figure 8 indicate that for a given Mach number, wing-rock onset occurred at approximately the same buffet intensity level regardless of wing flap configuration.

The subsonic wing-rock-onset data followed the same trend as the subsonic buffet-onset data. Up to the limits investigated, each increase in the deflection of either the leading- or the trailing-edge flap caused the C_{N_A} for wing-rock onset to rise. Transonically, however, with the leading-edge flap deflected, the wing-rock-onset boundary did not exhibit as rapid a decrease with increasing Mach number as did the buffet-onset boundary. With this more gradual decrease in wing-rock-onset boundary, the transonic (Mach numbers near 0.90) wing-rock-onset boundary showed an increase in C_{N_A} for each increase in leading- or trailing-edge flap deflection except for the 12° leading- and trailing-edge flap combination, for which the boundary dropped slightly. Transonically, the 7° leading-edge flap deflection in combination with the 12° trailing-edge flap deflection was equal to, or more effective than, the other flap combinations investigated in delaying wing-rock onset to a higher C_{N_A}.

In general, the C_{N_A} for wing-rock onset decreased as Mach number increased. At subsonic Mach numbers the leading-edge flap was more effective in raising the wing-rock-onset boundary than the trailing-edge flap. At the higher transonic Mach numbers investigated, however, the leading- and trailing-edge flaps appeared to be almost equally effective when deflected the same amount.

Pilot Comments

Pilot comments and impressions supported the data presented in this report and gave additional insight into the effects of wing flow separation. During the wind-up-turn maneuvers, the pilot noticed no appreciable difference in performance or handling qualities with the different wing flap combinations prior to the point of severe buffet intensity rise. At that point there was a definite increase in drag; however, the degradation of the handling qualities was not severe until the onset of wing rock which occurred at a higher angle of attack. The pilot felt that even small control inputs could induce wing-rock onset at angles of attack that were slightly lower than those recorded during these flights. Once wing rock was encountered, the only means the pilot had to recover was to reduce the airplane angle of attack.

The pilot's evaluation of the effects of various wing flap configurations agreed closely with the evaluation presented herein of the data from the aircraft instrumentation. Subsonically, the pilot gave the highest performance and handling qualities ratings to the wing flap configuration with 12° of leading-edge flap deflection and 12° of trailing-edge flap deflection. Transonically, the pilot felt that this configuration and the combination of 7° of leading-edge flap deflection with 12° of trailing-edge flap deflection were equivalent.

CONCLUSIONS

The effects of various combinations of leading- and trailing-edge flap deflections on buffet onset, wing-rock onset, and buffet loads were investigated at subsonic and transonic speeds during a flight-test program on an F-8C airplane. The principal findings of this investigation were:

(1) Subsonically, buffet onset, wing-rock onset, and buffet loads were delayed to a significantly higher airplane normal force coefficient by each increase in leading- or trailing-edge flap deflection up to the maximum deflection investigated (12°).

(2) Transonically, buffet onset, wing-rock onset, and equivalent values of buffet loads occurred at lower values of airplane normal force coefficient than at subsonic speeds. At the higher transonic speeds investigated (Mach numbers of approximately 0.90), the 7° leading-edge flap deflection combined with the 12° trailing-edge flap deflection was as effective as, or more effective than, the other leading- and trailing-edge flap combinations in delaying buffet onset, wing-rock onset, and buffet loads to a higher airplane normal force coefficient.

(3) Maximum wingtip accelerations of 5g to 6g were measured. However, these accelerations were at a relatively high frequency, and they did not result in large bending moments inboard on the wing. Maximum buffet loads measured inboard at the wing strain-gage station were approximately 10 percent of the 1g steady state flight bending-moment loads at the same location.

(4) The maximum buffet load attained for any wing flap configuration tested remained relatively constant even though the value of airplane normal force coefficient was greatly increased by the use of deflected flaps.

(5) The results of the frequency analysis of structural buffeting indicated that the wingtip experiences its highest power output at a frequency between the wing second bending and first torsional frequency and also responds with a lesser power at the wing first bending frequency. The response at the wing strain-gage location indicated significant power at only the wing first bending frequency.

(6) Wing-rock onset occurred at nearly the same buffet load values for all wing flap configurations at a given Mach number.

Flight Research Center,
National Aeronautics and Space Administration,
Edwards, Calif., April 12, 1973.

REFERENCES

1. Taylor, Robert T.: Recent Aerodynamic Studies Applicable to High Performance Maneuvering Aircraft. Conference on Aircraft Aerodynamics, NASA SP-124, 1966, pp. 89-103.

2. Friend, Edward L.; and Monaghan, Richard C.: Flight Measurements of Buffet Characteristics of the F-111A Variable-Sweep Airplane. NASA TM X-1876, 1969.

3. Fischel, Jack; and Friend, Edward L.: Preliminary Assessment of Effects of Wing Flaps on High Subsonic Flight Buffet Characteristics of Three Airplanes. NASA TM X-2011, 1970.

4. Friend, Edward L.; and Sefic, Walter J.: Flight Measurements of Buffet Characteristics of the F-104 Airplane for Selected Wing-Flap Deflections. NASA TN D-6943, 1972.

5. Mechtly, E. A.: The International System of Units — Physical Constants and Conversion Factors. NASA SP-7012, 1969.

6. Richardson, Norman R.; and Pearson, Albin O.: Wind-Tunnel Calibrations of a Combined Pitot-Static Tube, Vane-Type Flow-Direction Transmitter, and Stagnation-Temperature Element at Mach Numbers From 0.60 to 2.87. NASA TN D-122, 1959.

7. Davis, Harry J.; and Horn, Leon: Notes on the Use of Semiconductor Strain Gages. TR-1285, Harry Diamond Laboratories, Apr. 30, 1965. (Available from DDC as AD 615802.)

8. Sisk, Thomas R.: A Proposed Flight-Test Technique To Assess Fighter Aircraft Maneuverability. Air to Air Combat Analysis and Simulation Symposium, Tech. Rep. AFFDL-TR-72-57, Vol. I, May 1972, pp. 339-361.

9. Damstrom, E. K.; and Mayes, J. F.: Transonic Flight and Wind Tunnel Buffet Onset Investigation of the F-8D Aircraft - Analysis of Data and Test Techniques. AIAA Paper No. 70-341, 1970.

TABLE 1. — F-8C WING PHYSICAL CHARACTERISTICS

Wing —	
Airfoil section, root	NACA 65A006
Airfoil section, tip	NACA 65A005
Span, m (ft)	10.87 (35.67)
Area, m^2 (ft^2)	34.84 (375)
Sweep (quarter chord), deg	42
Aspect ratio	3.4
Taper ratio	0.247
Leading-edge flap —	
Area, per side, m^2 (ft^2):	
Inboard section	2.03 (21.9)
Outboard section	1.28 (13.8)
Chord, percent wing chord:	
Inboard	20
Outboard	32
Spanwise location, percent semispan:	
Inboard end —	
Inboard section	12.3
Outboard section	63.0
Outboard end —	
Inboard section	63.0
Outboard section	100.0
Trailing-edge flap —	
Area, per side, m^2 (ft^2)	1.93 (20.78)
Chord, percent wing chord	25.7
Spanwise location, percent semispan:	
Inboard end	22.2
Outboard end	62.6

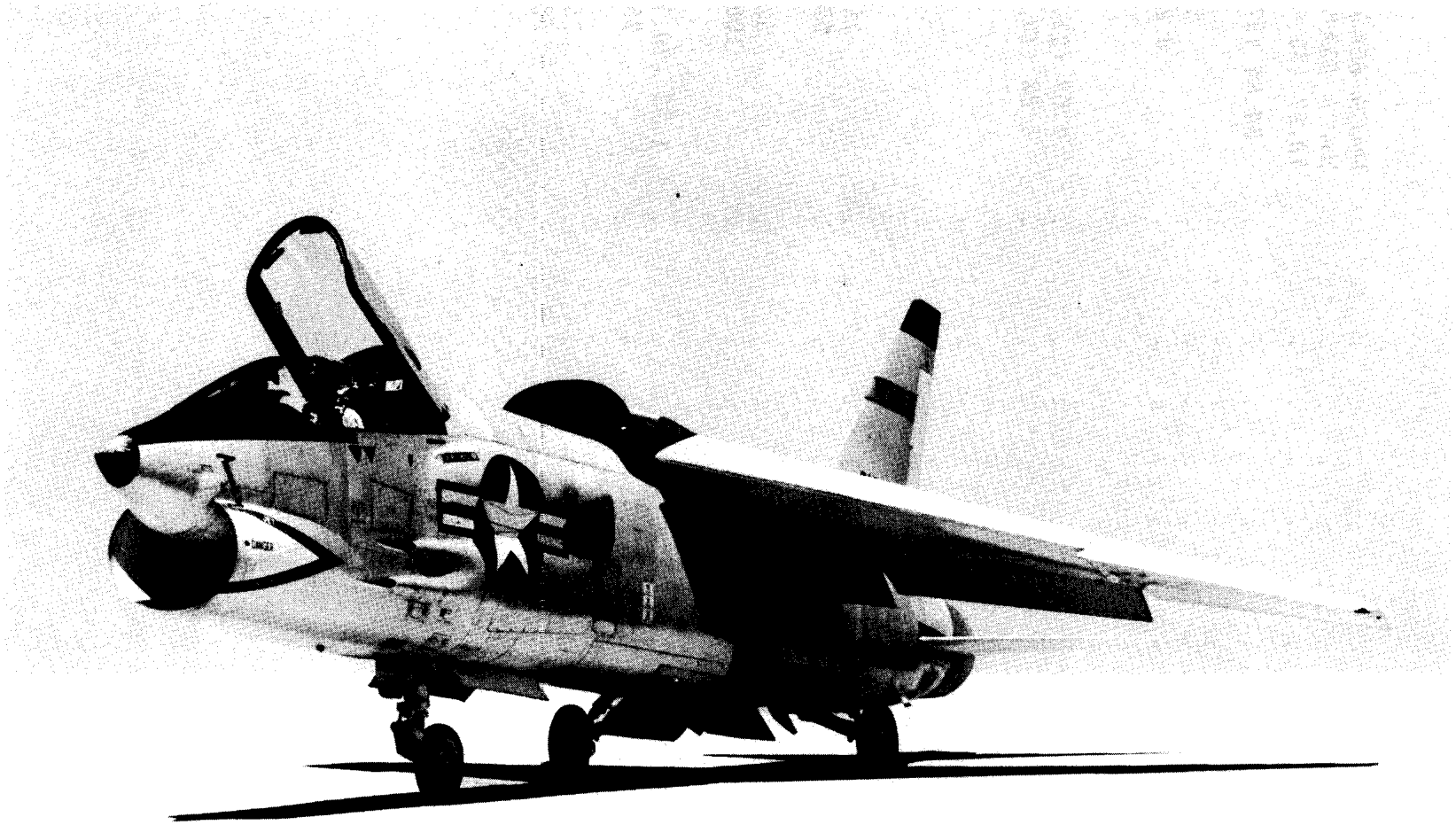

Figure 1. F-8 airplane.

E-20089

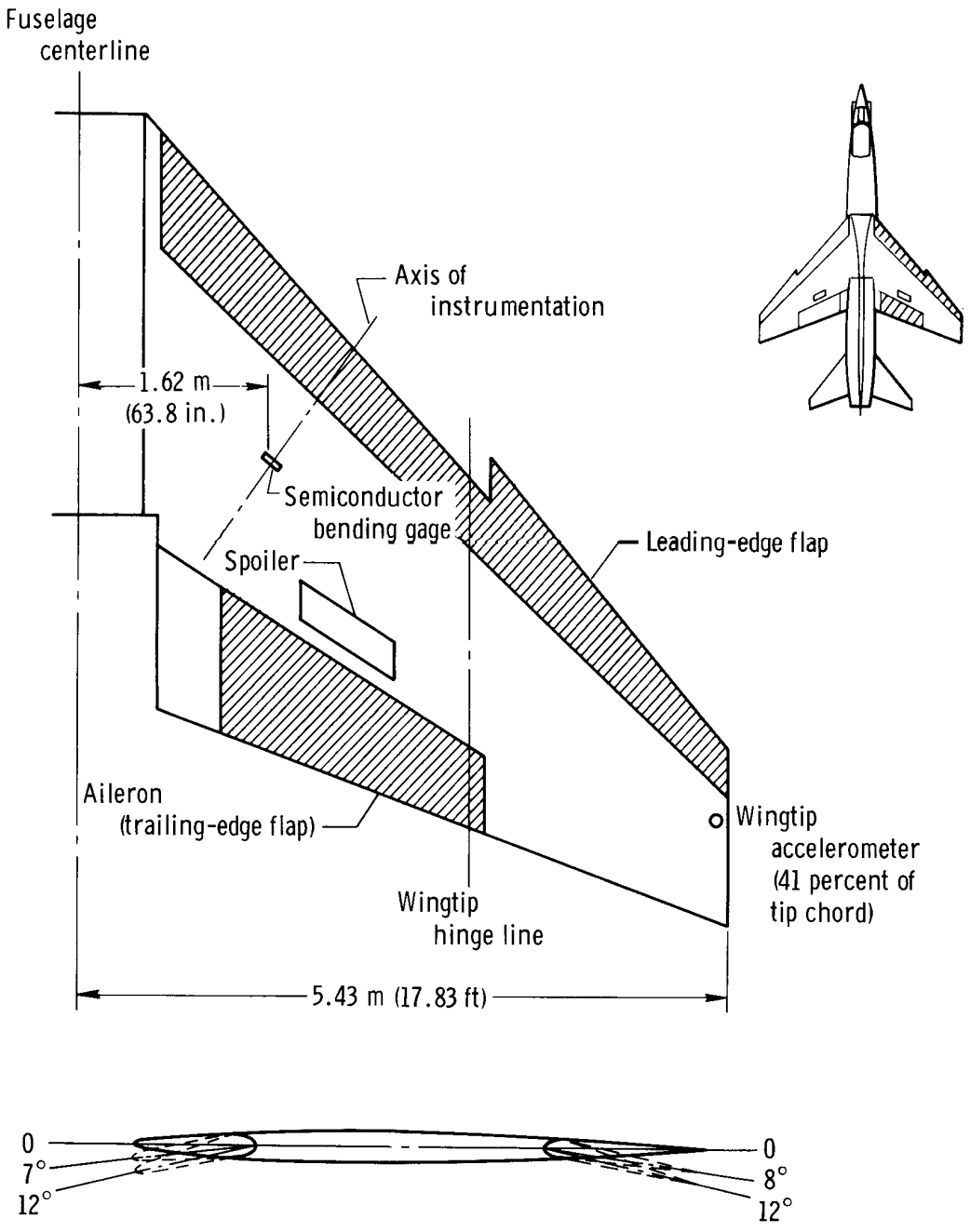

Figure 2. F-8C wing and wing instrumentation.

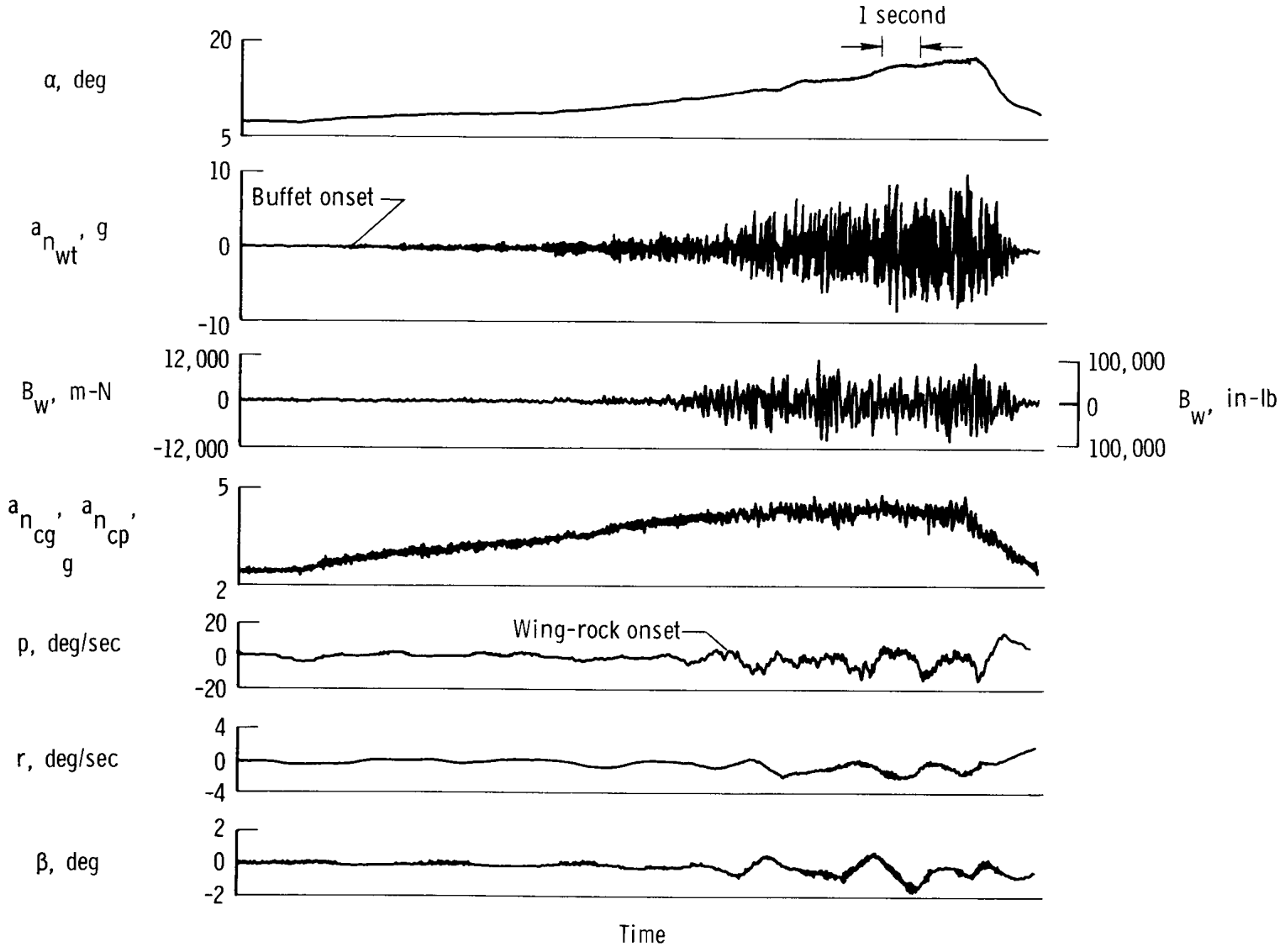

Figure 3. Time history of a typical wind-up-turn maneuver.

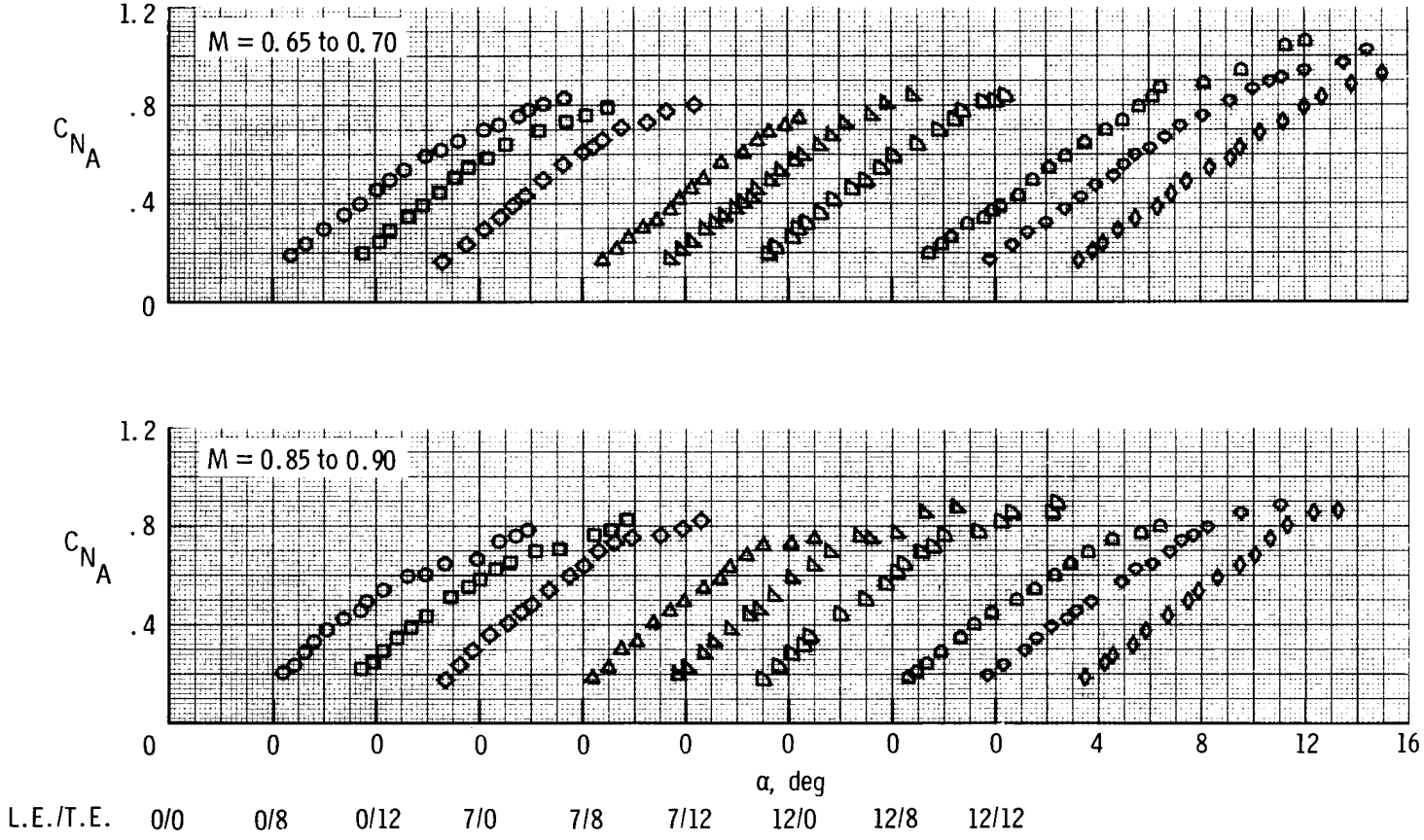

Figure 4. Airplane normal force coefficient as a function of angle of attack for subsonic and transonic Mach numbers.

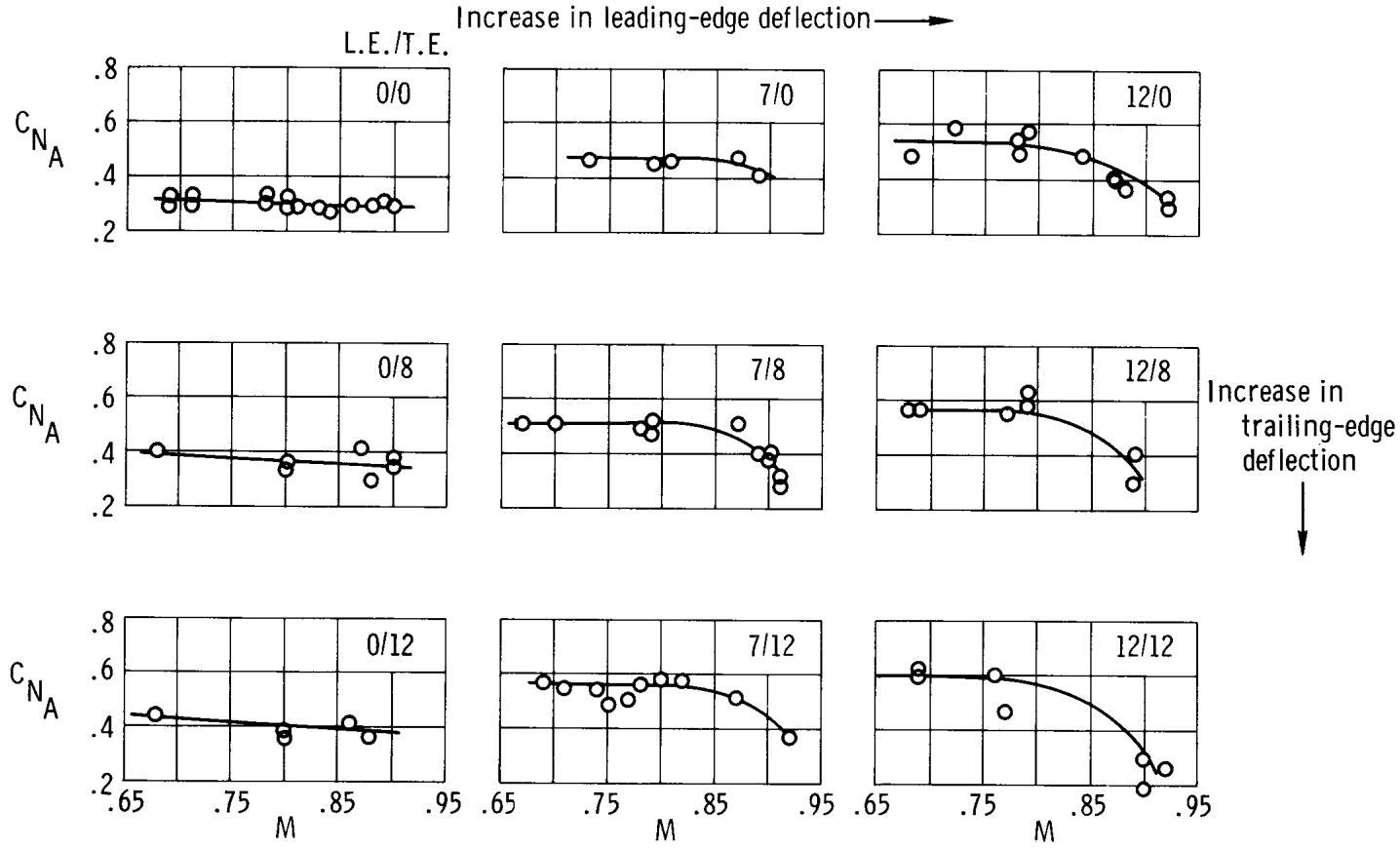

Figure 5. Buffet-onset boundaries for nine combinations of leading- and trailing-edge flap deflections.

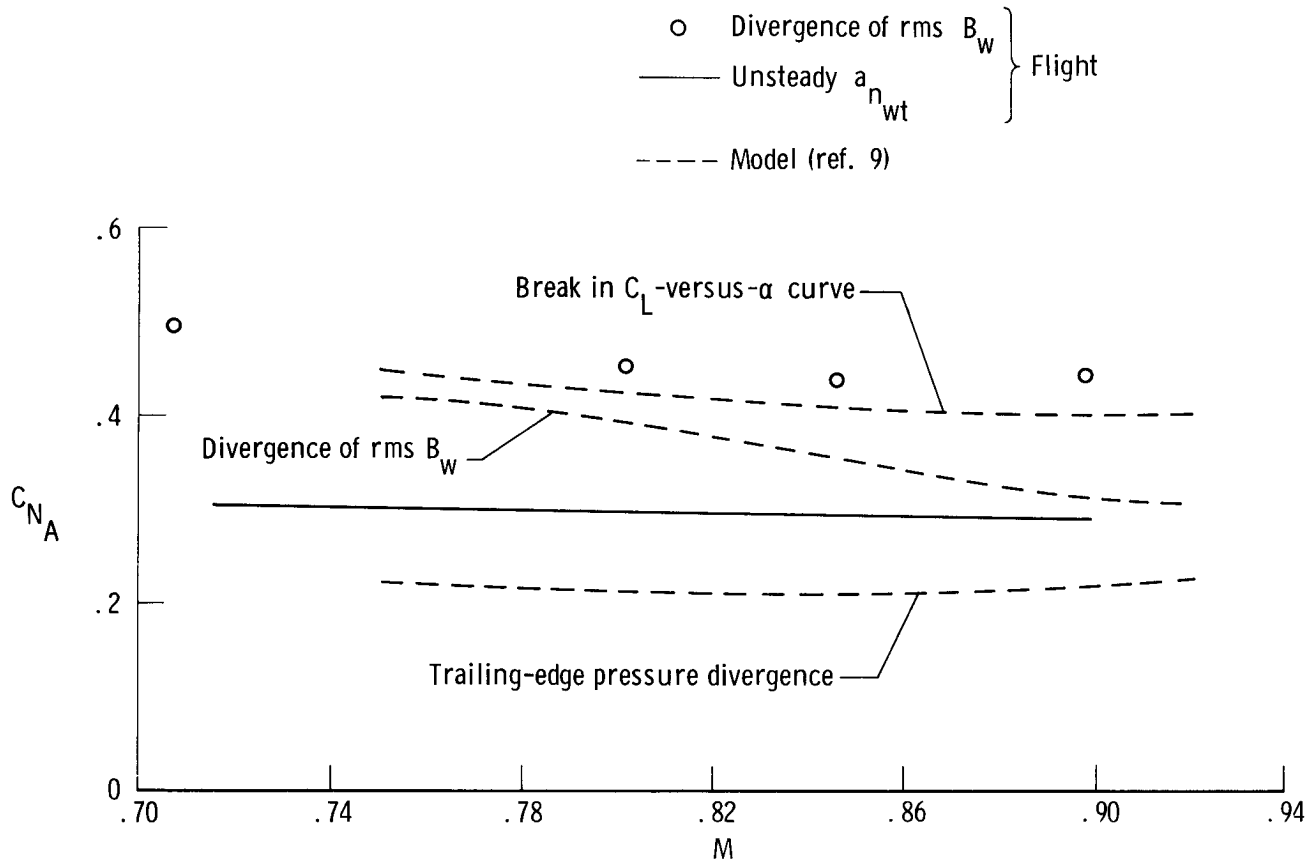

Figure 6. Values of C_{N_A} for several buffet-onset criteria applied to a 0.042-scale model of the F-8 and the F-8C airplane. Clean-wing configuration.

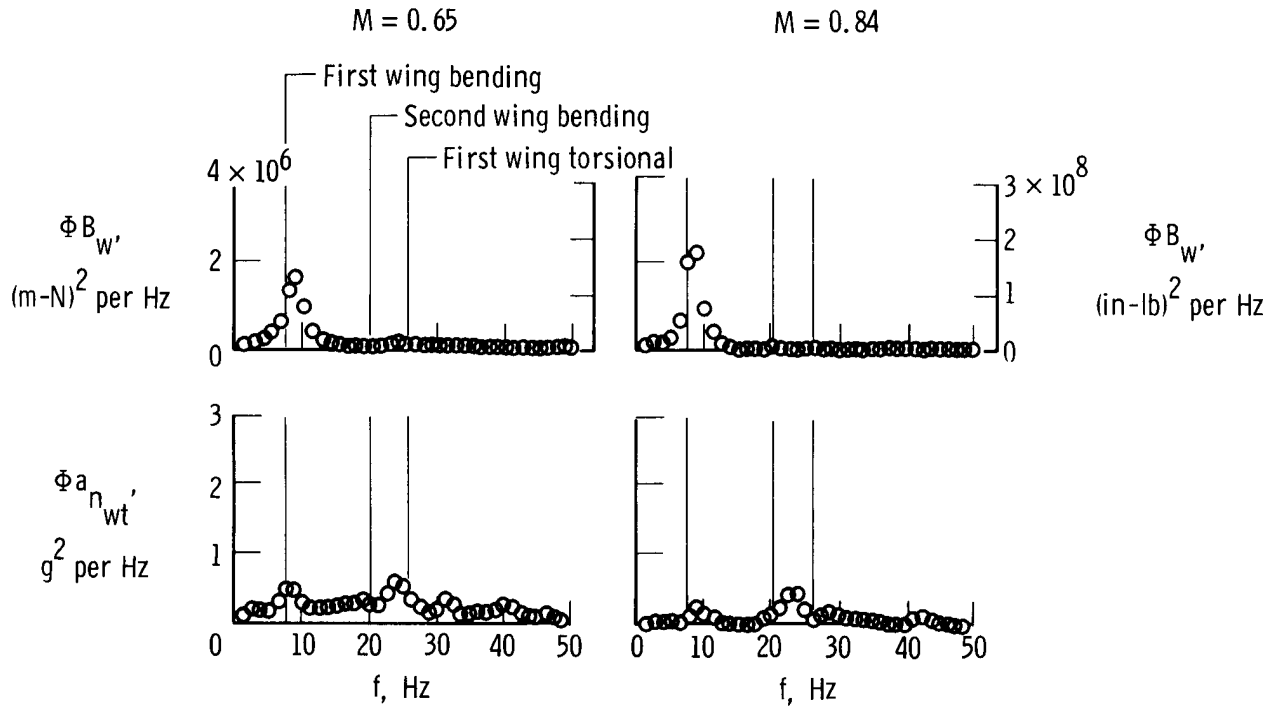

(a) L.E./T.E. = 0/0.

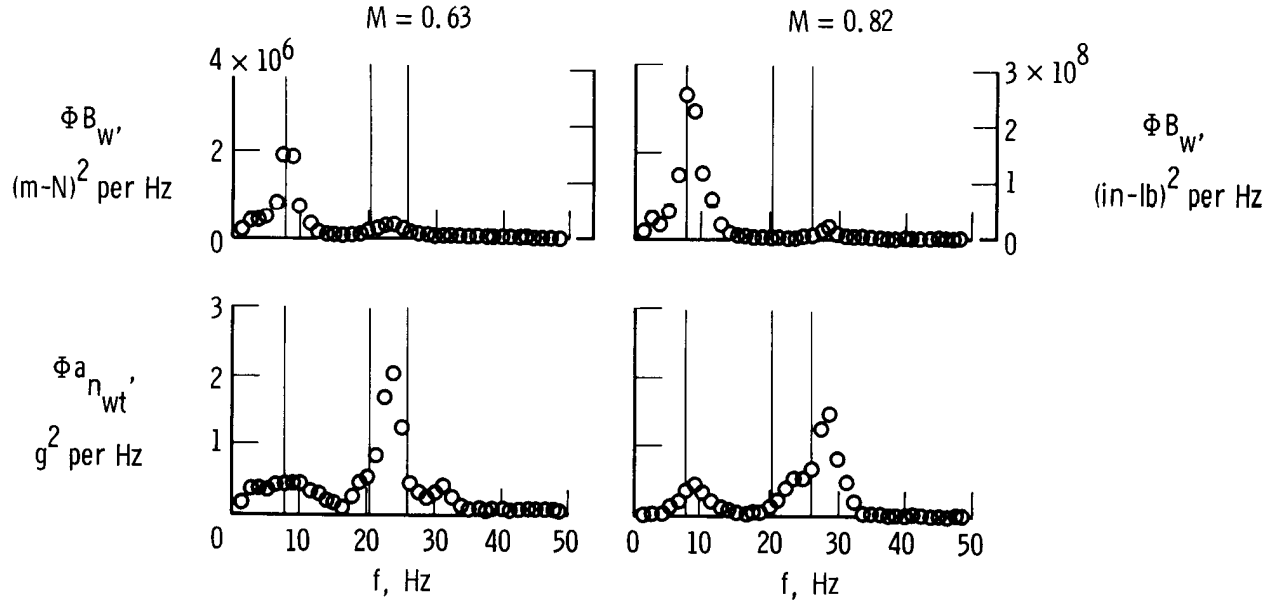

(b) L.E./T.E. = 7/12.

Figure 7. Power spectral density for subsonic and transonic flight at three wing flap configurations.

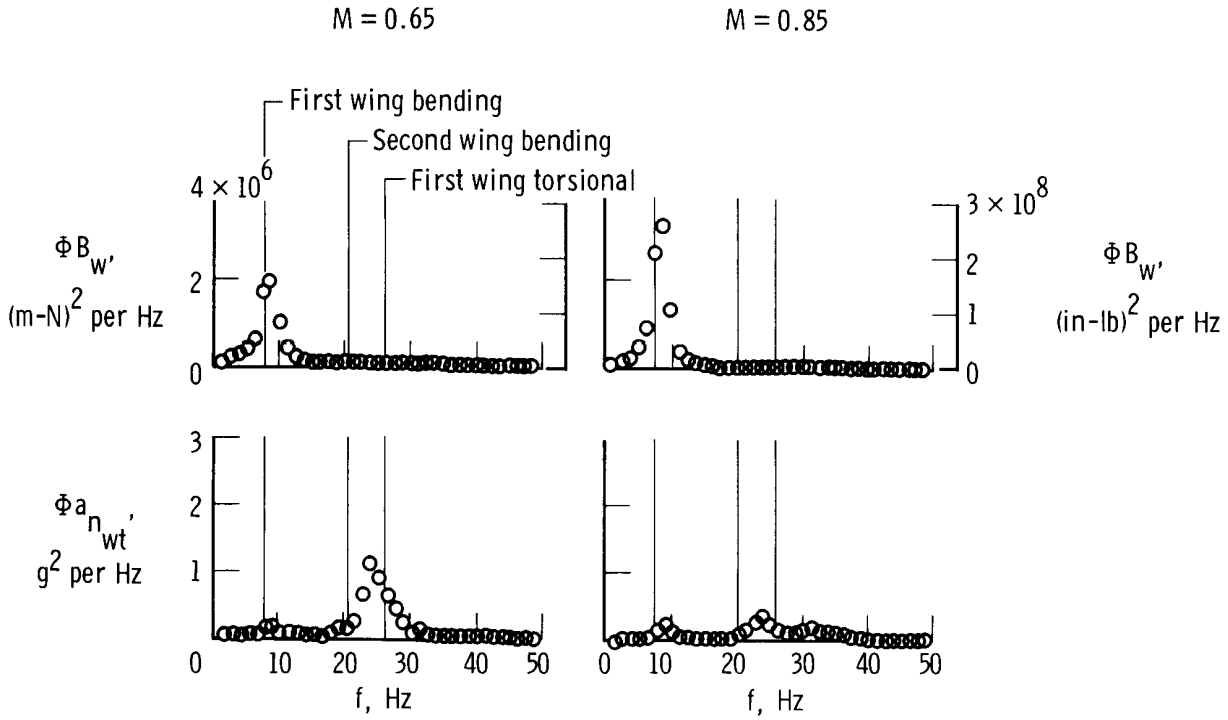

(c) L.E./T.E. = 0/12.

Figure 7. Concluded.

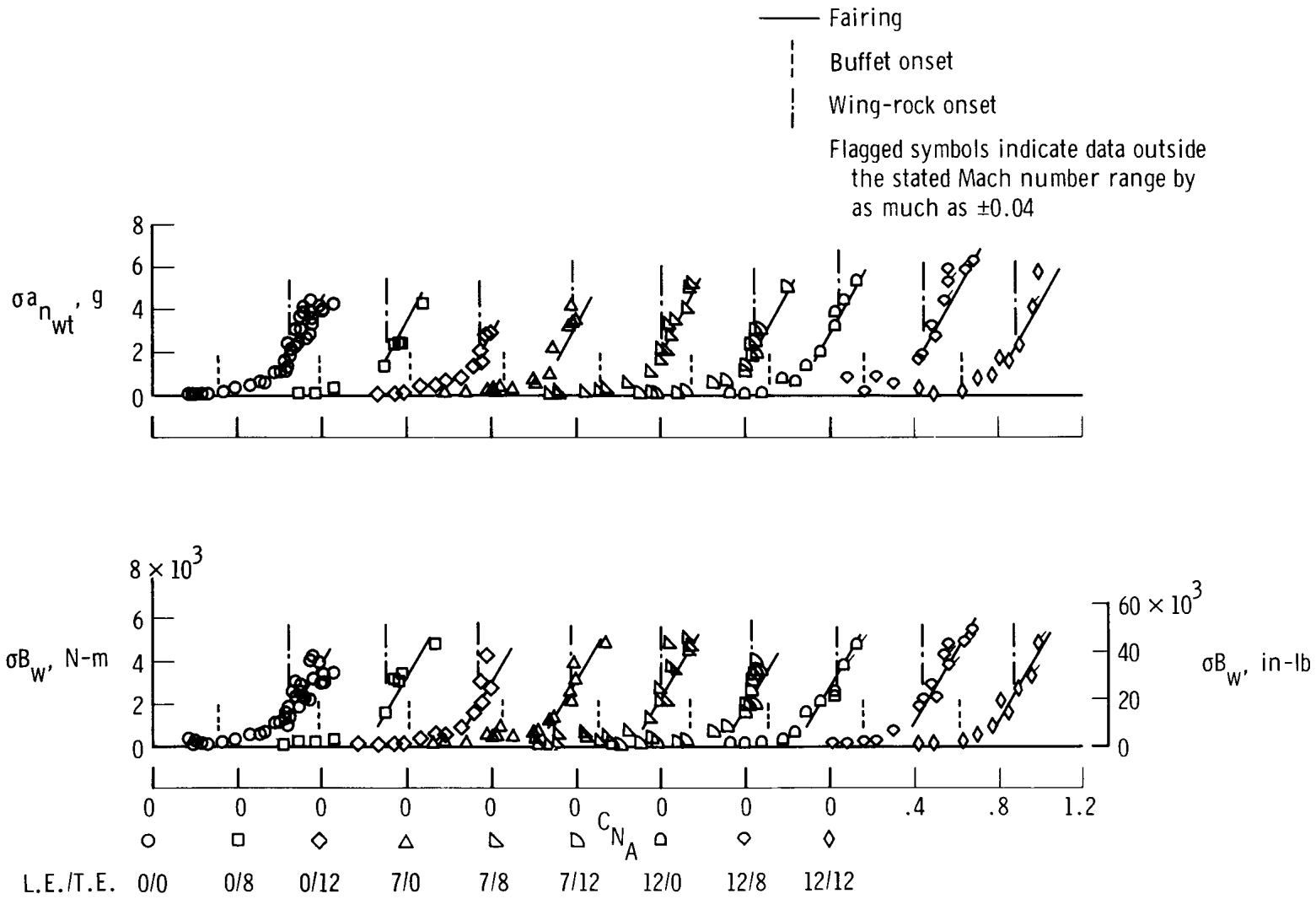

(a) Subsonic Mach numbers (0.65 to 0.70).

Figure 8. Summary of rms buffet load data for subsonic and transonic Mach numbers.

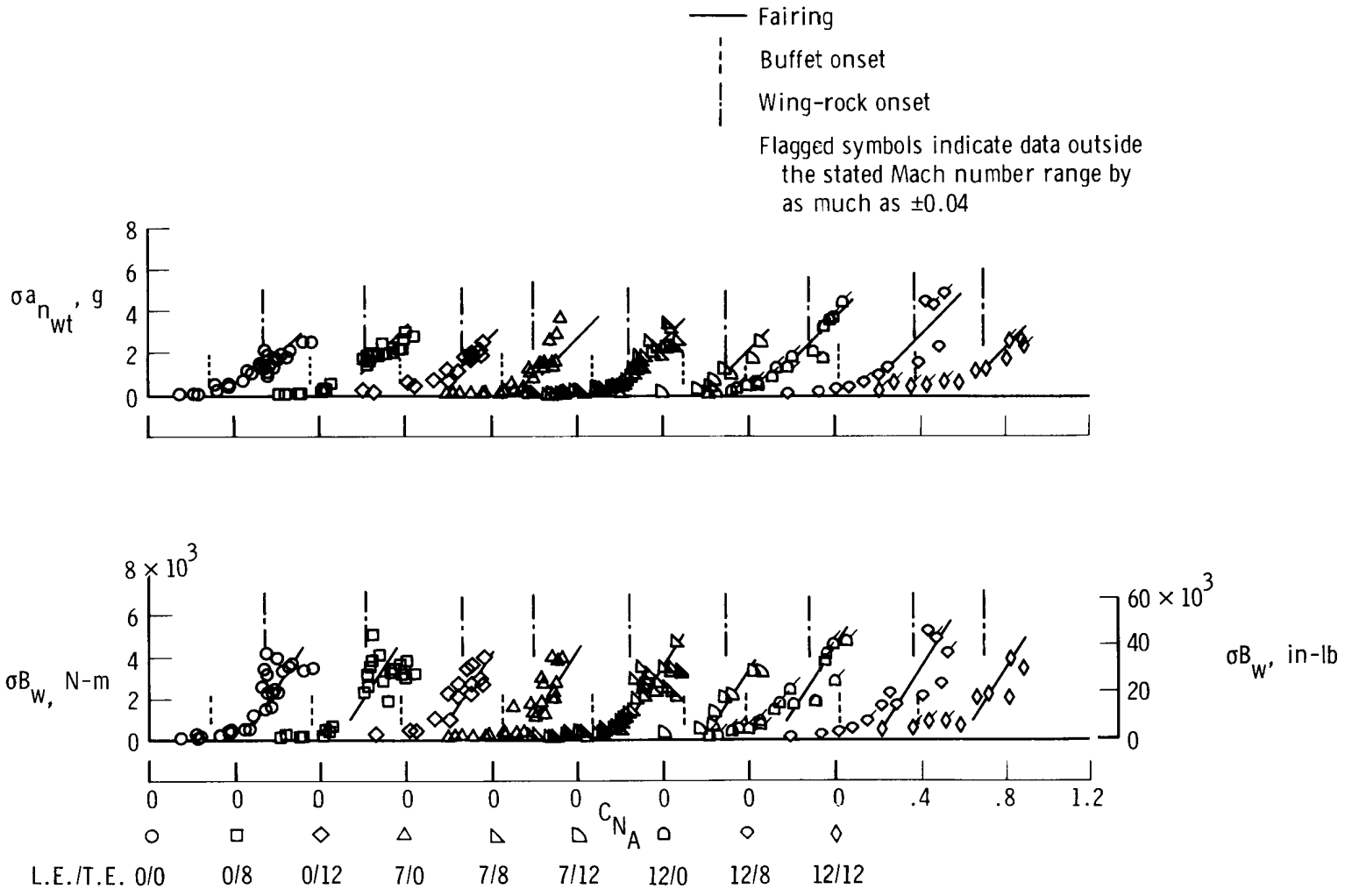

(b) Transonic Mach numbers (0.85 to 0.90).

Figure 8. Concluded.

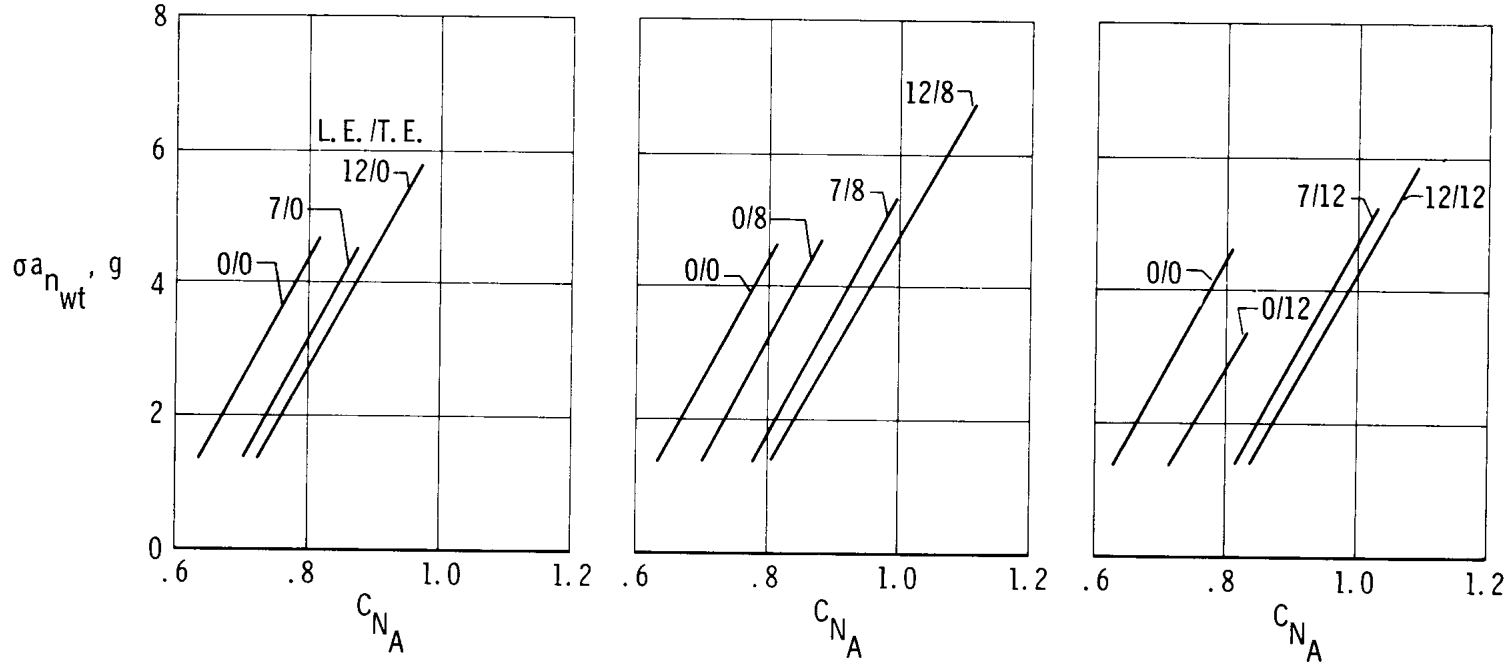

(a) Subsonic Mach numbers (0.65 to 0.70).

Figure 9. Comparison of subsonic and transonic buffet loads for the range of wing flap configurations investigated.

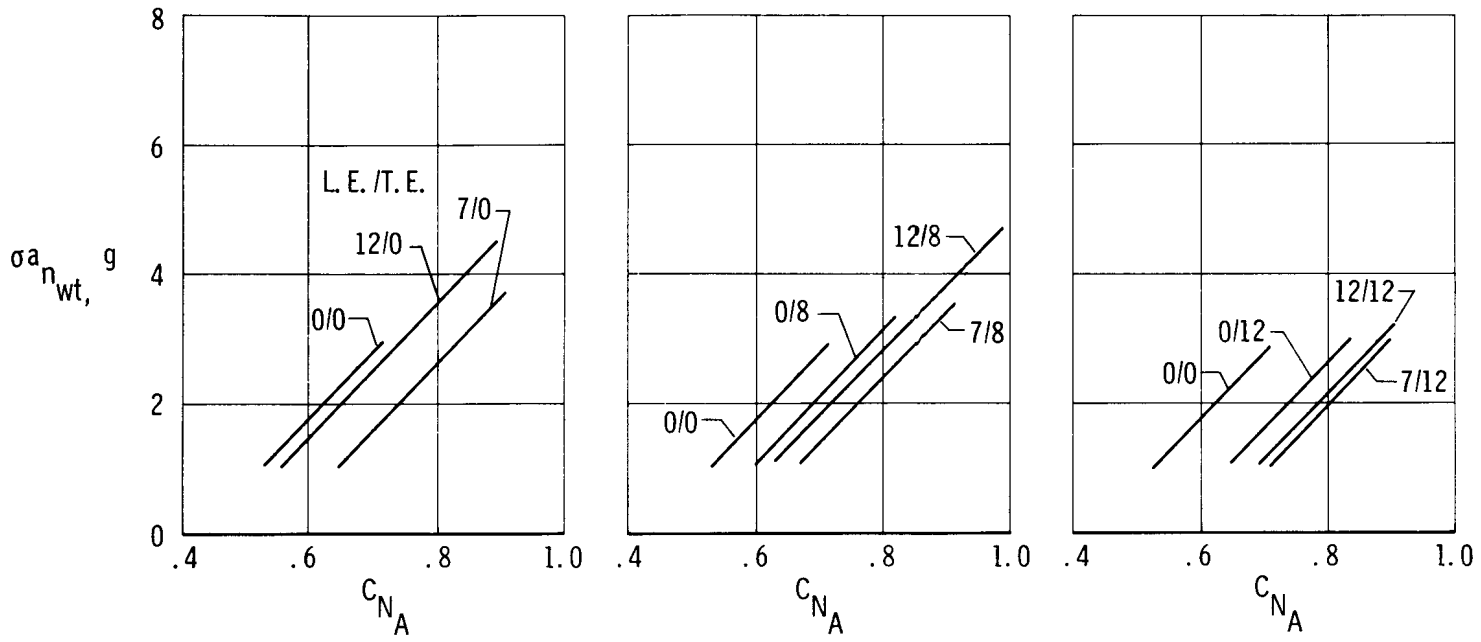

(b) Transonic Mach numbers (0.85 to 0.90).

Figure 9. Concluded.

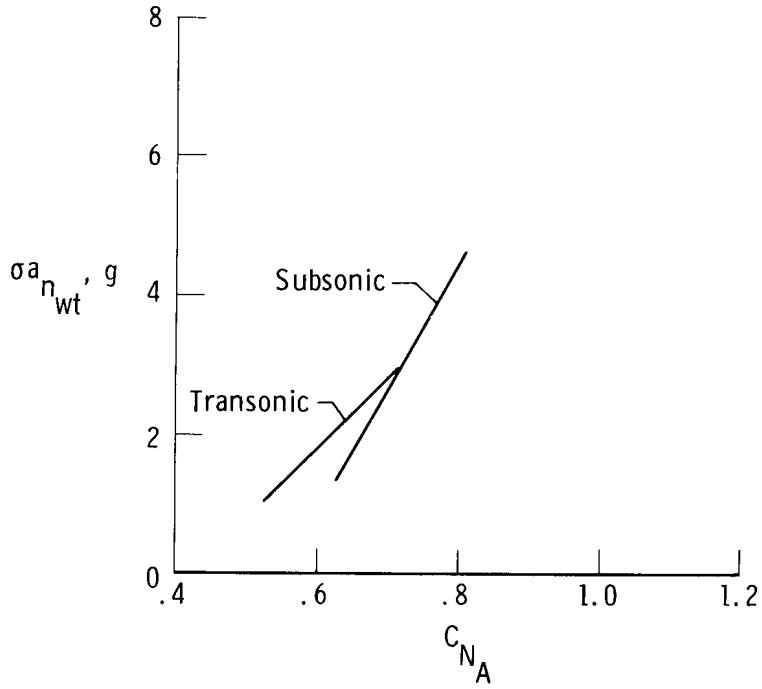

(a) L.E./T.E. = 0/0.

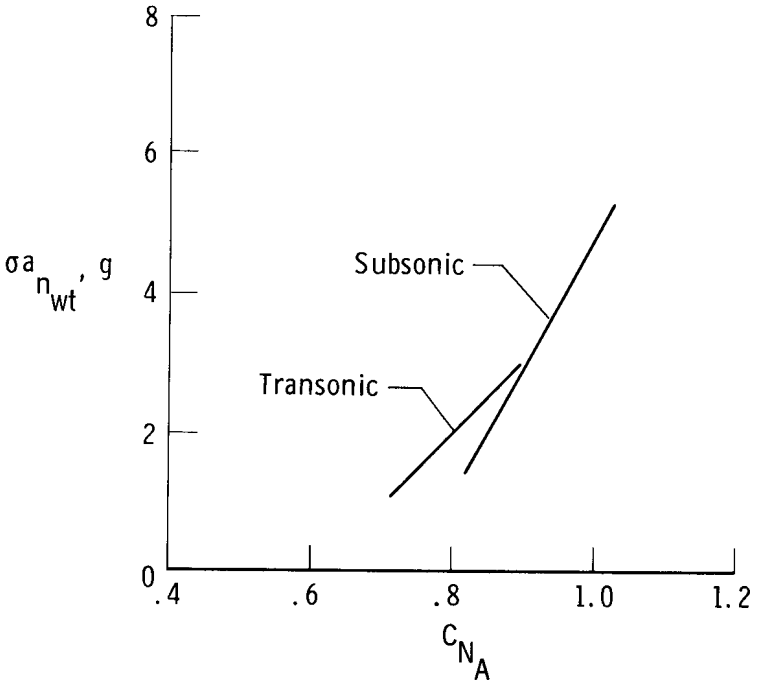

(b) L.E./T.E. = 7/12.

Figure 10. Comparison of the buffet intensity rise at subsonic Mach numbers with that at transonic Mach numbers.

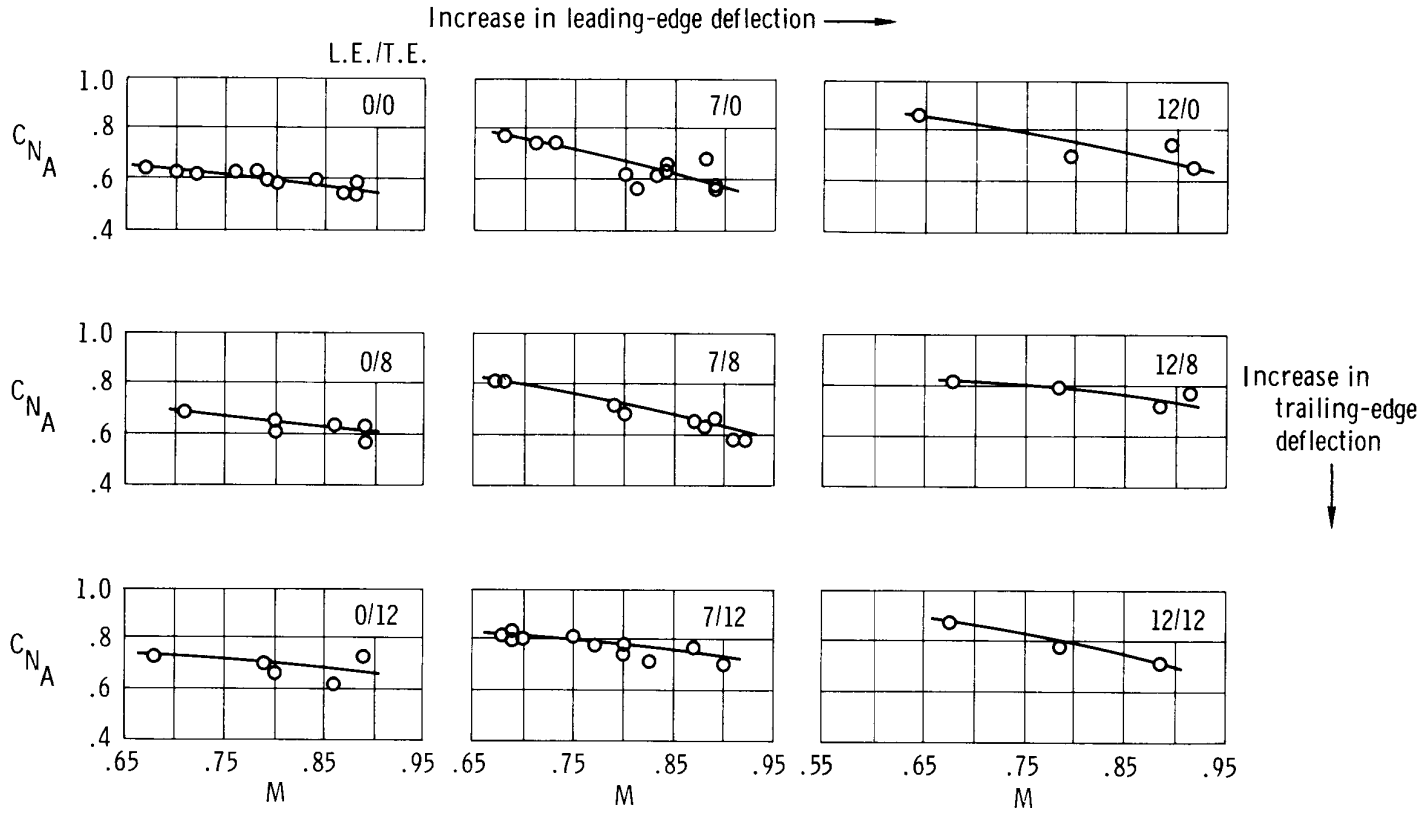

Figure 11. Wing-rock-onset boundaries presented as C_{N_A} versus Mach number for nine combinations of leading- and trailing-edge flap deflections.